

RSC Advances



This is an *Accepted Manuscript*, which has been through the Royal Society of Chemistry peer review process and has been accepted for publication.

Accepted Manuscripts are published online shortly after acceptance, before technical editing, formatting and proof reading. Using this free service, authors can make their results available to the community, in citable form, before we publish the edited article. This *Accepted Manuscript* will be replaced by the edited, formatted and paginated article as soon as this is available.

You can find more information about *Accepted Manuscripts* in the [Information for Authors](#).

Please note that technical editing may introduce minor changes to the text and/or graphics, which may alter content. The journal's standard [Terms & Conditions](#) and the [Ethical guidelines](#) still apply. In no event shall the Royal Society of Chemistry be held responsible for any errors or omissions in this *Accepted Manuscript* or any consequences arising from the use of any information it contains.



Journal Name

ARTICLE

New Iodonium Salts in NIR Sensitized Radical Photopolymerization of Multifunctional Monomers†

Thomas Brömme, Dennis Oprych, Joachim Horst, Paula Sevenini Pinto, Bernd Strehmel*

Received 00th January 20xx,
Accepted 00th January 20xx

DOI: 10.1039/x0xx00000x

www.rsc.org/

Reactivity of new iodonium salts $[\mathbf{A-I-B}]^+\mathbf{X}^-$ was studied with near infrared (NIR) initiated radical polymerization by photo-DSC using the polymethine dye **S1** (5-(6-(2-(3-Ethyl-1,1-dimethyl-1H-benzo[e]indol-2(3H)-ylidene)ethylidene)-2-(2-(3-ethyl-1,1-dimethyl-1H-benzo[e]indol-3-ium-2-yl)vinyl)cyclohex-1-en-1-yl)-1,3-dimethyl-2,6-dioxo-1,2,3,6-tetrahydropyr-imidin-4-olate) as sensitizer. The iodonium salt $[\mathbf{A-I-B}]^+\mathbf{X}^-$ functioned as radical initiator bearing a different substitution pattern of the cation and the anion, respectively. Electron transfer of the excited state of **S1** to $[\mathbf{A-I-B}]^+\mathbf{X}^-$ (\mathbf{X}^- : benzilate, lactate, NO_3^- , PF_6^- , SbF_6^- , $p\text{-CH}_2=\text{CH-Ph-SO}_3^-$, $p\text{-C}_{12}\text{H}_{15}\text{-Ph-SO}_3^-$, CF_3SO_3^- , $\text{C}_4\text{F}_9\text{SO}_3^-$, $\text{B}(\text{CN})_4^-$, $\text{B}(\text{Ph})_4^-$, $\text{B}(\text{PhF}_3)_4^-$, $\text{N}(\text{CN})_2^-$, $(\text{SO}_2\text{-CF}_3)_2\text{N}^-$) results in initiating radicals. Reactivity of $\mathbf{S1}/[\mathbf{A-I-B}]^+\mathbf{X}^-$ correlated with conductivity of the salt in acrylate monomers such as hexane-1,6-diol diacrylate, tripropylene glycol diacrylate, poly(ethylene glycol) diacrylate and trimethylolpropane triacrylate. A high conductivity related always to a better reactivity in the monomer chosen. The solubility of $[\mathbf{A-I-B}]^+\mathbf{X}^-$ determined ranges between several $\text{g}\cdot\text{L}^{-1}$ up to well mixable systems ($>2000\text{ g}\cdot\text{L}^{-1}$). Particular the bis(trifluoromethylsulfonyl) imide anion $(\text{N}(\text{SO}_2\text{-CF}_3)_2)^-$ resulted in giant solubilities depending on the $[\mathbf{A-I-B}]^+$ cation. A high solubility did not always lead to a high reactivity. Furthermore, iodonium salts comprising the bis(trifluoromethylsulfonyl) imide anion exhibited a lower cytotoxicity compared to those with the tetraphenyl borate anion as determined by the MTT-test using CHO-9-cells.

Introduction

Near-infrared (NIR) sensitized photopolymerization has been still in its infancy. The first commercially used patent with focus on NIR exposure was released in 2000¹ while the number of fundamental publications regarding this topic represented a small level at this time. This technique was developed in industry using NIR-lasers for exposure². The development of laser techniques emitting in the NIR with focus on 808 nm or 830 nm has brought new exposure techniques to praxis; that is digital imaging based on the Computer to Plate (CtP) technology². Today's commercialized CtP systems based on photoinitiated polymerization operating either at 808 nm or 830 nm exhibit a sensitivity between 50-200 mJ/cm^2 depending on processing conditions^{2c}. They use a redox-based photoinitiator (PI) comprising a NIR-dye as sensitizer (Sens) and a radical initiator (RI). The latter is either an iodonium³ salt or triazine⁴. Both RIs have been known in photopolymer systems based on UV or visible light excitation. A

comprehensive overview about this field is available⁵. The introduction of PIs based on UV-excitation has brought many applications to the market⁶. Although this technique offers many features, it also has some disadvantages. This is the incorporation of either UV protecting materials or additives in general with remarkable UV absorption.

Electron transfer builds the main driving source to generate initiating radicals in NIR photopolymerization either. The first excited singlet state of Sens transfers an electron to RI resulting in formation of initiating radicals. This combination results in a slight negative free enthalpy of photoinduced electron transfer (ΔG_{el})^{2c}. Thus, one could expect similar initiation efficiencies. However, our result showed an influence even of redox-inactive anions on photopolymer reactivity. Furthermore, generation of initiating radicals based on NIR exposure mainly bases on electron transfer, the individual occurring steps may differ compared the UV systems. Thus, thermal energy would be additionally released as result of thermal deactivation. This is the major deactivation pathway occurring in cyanine dyes with absorption $>750\text{ nm}$. Physical processes in the coating needed for film formation may benefit from such processes and the heat released may accelerate chemical processes either. Moreover, NIR light also possesses a deeper penetration into biological samples with embedded collagen in the matrix. Thus, these exposure sources might be helpful to expose biological materials. Furthermore, irradiation of cells with NIR-radiation may result in less cell damage compared to UV light.

Niederrhein University of Applied Sciences, Department of Chemistry and Institute for Coatings and Surface Chemistry, Adlerstr. 32, D-47798 Krefeld, Germany, e-mail: bernd.strehmel@hsnr.de

† Electronic Supplementary Information (ESI) available: procedures for synthesis of iodonium salts and reactivity data, See DOI: 10.1039/x0xx00000x

Surprisingly, NIR-photopolymers have not been used in industrial coating systems yet although a feasibility study approved their working principle⁷. Economic reasons may limit application of such redox based PIs on the one hand but it has been also well accepted that the solubility limits their use in high viscous industrial coatings. Iodonium tetraphenylborates have been mostly used as RI in NIR-based CTP systems^{2c}. Nevertheless, the modest compatibility of iodonium tetraarylborates with high viscous industrial coatings limits their use outside of the graphic industry.

As a consequence, there exists a demand to use iodonium salts exhibiting a better solubility in industrial coatings not only for NIR applications. This study shows a new approach to improve the solubility of iodonium salts in coatings by introducing of alternative weak coordinating anions ($[(CF_3SO_2)_2N]^-$) on the one hand and change of substitution pattern at the cation on the other hand. These new iodonium salts result in a better solubility and reactivity compared to commercially available iodonium salts bearing either $B(Ph)_4^-$, PF_6^- or SbF_6^- . Hexafluorophosphates in general may arise additional problems regarding the release of HF under certain circumstances⁸ while the substitution of antimony has been an issue as well⁹.

Moreover, we tried to find out correlations between reactivity and solubility. This failed in many examples while a correlation exists between reactivity and conductivity of the iodonium salt in the coating showing that dissociation into the single solvated separated ions controls the reactivity. This surprises because it has been believed that redox inactive anions should not significantly influence the reaction steps resulting in initiating radicals. Furthermore, cytotoxicity experiments demonstrate the less toxic behaviour of iodonium salts bearing the bis(trifluoromethylsulfonyl)imide anion compared to those with tetraphenyl borate as counter ion.

Experimental

General information

Materials, chemicals and solvents. Hampford Research donated the Iodonium salts **1g** (FP5034), **1h** (FP5035), **1i** (FP5033), **8g** (FP5384) and **8h** (FP5386). The iodonium salt **4b** (IO591) was purchased from TCI. The anions $C_4F_9SO_3^-$ and Bis(trifluoromethylsulfonyl)imide were bought from IoLITec as potassium and lithium salt, respectively. Potassium tetracyanoborate ($K[B(CN)_4]$) was obtained from SelectLab Chemicals. All other anions shown in Scheme 3 were purchased from Sigma Aldrich. FEW Chemicals GmbH donated the NIR-dye **S 2265 (S1)**. NMR solvents were obtained from Armar Chemicals. The monomers 1,6 hexanediol diacrylate (**M1**), tripropylene glycol diacrylate (**M2**), polyethylene glycol (600) diacrylate (**M3**), and trimethylolpropane triacrylate (**M4**) were received from Sartomer as scientific gift and used without further treatment. Supporting information contains a summary of non-commercially available iodonium salts.

Equipment. **NMR:** A Fourier 300 from Bruker was used for all NMR-measurements. 5-20 mg and 50-100 mg sample were

dissolved in 0.7 mL solvent for 1H -NMR and ^{13}C -NMR measurements, respectively. **MS:** ESI spectra were taken using a LXQ-linear ion trap from Thermo Fischer Scientific to determine the molecular weight of the cations and anions in positive and negative mode, respectively. **GC-MS** was applied to determine the solubility of the iodonium salts using an Agilent Technologies 7890A for the GC, an Agilent Technologies 5975C inert XL MSD with Triple-Axis Detector as MS-Detector, and a Gerstel Multi Purpose Sampler MPS2 as Autosampler. **FTIR:** Data were measured with a Bruker alpha FTIR applying ATR technique for spectral recording. **UV-Vis-NIR:** This was taken with a Cary 5000 from Agilent in 1 cm cuvettes. **Conductivity:** These measurements were carried out with a 856 conductivity module with Conductivity measuring cell (stainless steel, $c = 0.1\text{ cm}^{-1}$, Pt1000) and 900 touch control from Metrohm. **Cytotoxicity:** A GENios Microplate Reader from Tecan was used for cytotoxicity measurements. Colorimetric measurements were applied for MTT-test¹⁰.

Procedures

Solubility of the iodonium salts. The solubility of the Iodonium salts was determined with GC-MS. The salt quantitatively decomposes $>230^\circ\text{C}$. Sample preparation started with stepwise dissolution of the salt in the monomer (starting with 50mg salt in 500 μL monomer, the amount of iodonium salt was increased with 50mg steps until the monomer was oversaturated with the salt, which can be visually seen by the appearance of two phases). The solution was transferred in an ultrasonic bath for 10 min, and centrifuged to separate the non-dissolved iodonium salt. The liquid phase was finally filtered to obtain the saturated monomer solution. Subsequently, the solution obtained was diluted with methanol (Merck) resulting in a concentration of $0.25\text{-}1\text{g}\cdot\text{L}^{-1}$. This defined solution was transferred to the GC-MS where it was injected into the injector, with a cold application. The injection temperature was set at 30°C and increased after 0.05 min isothermal driving to 320°C applying a heating range of $12^\circ\text{C}\cdot\text{s}^{-1}$. Finally, the iodonium salt was separated on a DP-5ms column (30 m in length; $0.25\text{ }\mu\text{m}$ film thickness; 0.25 mm inner diameter) with a constant flow rate of 1 ml/min (Agilent). The initial oven temperature was set at 50°C . It was increased after 3 min isothermal keeping to 150°C with a rate of $30^\circ\text{C}\cdot\text{min}^{-1}$. Afterwards, it was furthermore applying a heating rate of $15^\circ\text{C}\cdot\text{min}^{-1}$ up to the final temperature at 320°C where it was hold for two min. Helium was used as carrier gas. The transfer line was set at 250°C . These conditions resulted in a complete thermal decomposition of the iodonium salt into the corresponding aryl iodide as identified in the mass spectrum. This was quantified using defined concentrations of iodonium salt, which were injected into GC-MS equipment resulting a calibration curve for each iodonium salt.

Photopolymerization. A regular photo-DSC setup was used to determine the photo initiation efficiency of the NIR photoinitiator systems in the monomers. Each sample went through a syringe filter before used in the experiment. A NIR-LED-array (LED790-66-60 from Roithner) emitting at 778 nm

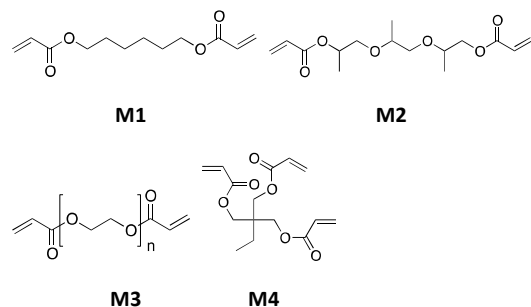
was used for all exposure experiments (output 1W). The light generated was collected with a lens and projected into a γ -fiber, which was connected with the head of the DSC (Q2000 from TA-Instruments). The output of each fibre arm was adjusted at the γ -fibre with a strong emitting source (OmniCure HR4000 from TA-Instruments, coupled additionally to the DSC). This realizes an almost equal intensity of each fibre arm being available for simultaneous exposure of both the sample and reference in the calorimeter. The LED-source was synchronized with the DSC by a shutter system placed between the fiber and the lens. It was controlled by an Arduino uno board, which was programmed with the program Arduino 1.05 available from Arduino. The software of the DSC controls the event-output of this instrument functioning as digital switch. Change of resistance resulted in an ON(no resistance)/OFF (infinite resistance) modulation. This information goes to the Arduino uno board controlling the shutter in ON/OFF position by a servomotor. Supporting information provides more details regarding the setup. Sensitizer concentration was 0.83 mM in **M1**, 0.85 mM in **M2**, 0.92 mM in **M3** and 0.9 mM in **M4**. Iodonium salt concentration was 15 mM in **M1**, 15.4 mM in **M2**, 16.6 mM in **M3** and 16.3 mM in **M4**.

Conductivity of the iodonium salts in the monomers. Conductivity was measured at different concentrations; that is 0.1 mM, 0.4 mM, 1.6 mM, 3.6 mM and 10 mM with three replicates. The cell constant was determined using an aqueous KCl solution daily and by each change of the monomer.

Results and Discussion

Materials and light source selection

The monomers **M1-M4** were selected to study the reactivity of the NIR photoinitiator systems. They exhibit both a different functionality and polarity resulting in distinct crosslinked polymeric materials after exposure. In this series, **M4** possesses the highest functionality while **M1-M3** bear the same number of double bonds in the monomer. **M3** exhibits the highest polarity followed by **M2** and **M1**.



A combination of a polymethine dye (sensitizer) and a radical initiator, an iodonium salt, was selected as photoinitiator system. The polymethine structure **S1** possesses as a neutral polymethine dye an acceptable solubility in the monomers **M1-M4**¹¹. On the other hand, we also tested commercially available cationic dyes regarding their function

as sensitizer in our systems¹². These dyes were significantly less sensitive in our formulations and they exhibited a less dissolution in the monomers **M1-M4**. Therefore, focus was kept on **S1**.

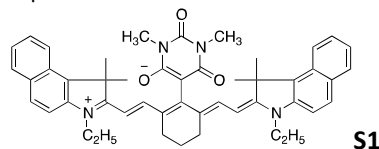


Figure 1 compares the absorption spectrum of **S1** taken in **M1** ($\lambda_{\max} = 786$ nm) with the spectral shape of a NIR LED-array showing an emission centre at $\lambda_{\max} = 778$ nm. An almost satisfied overlap exists between **S1** absorption and LED-emission.

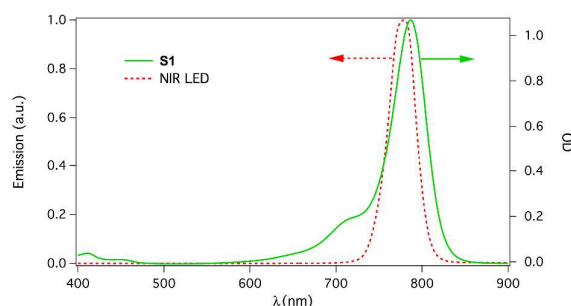


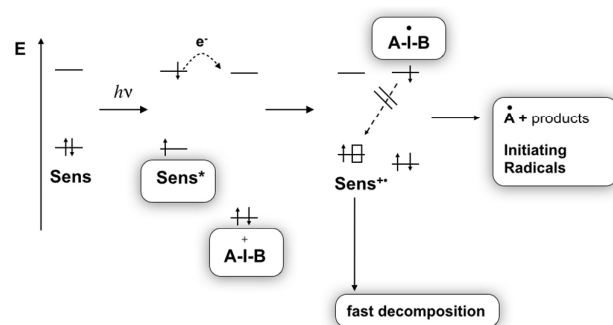
Figure 1: Spectral comparison of **S1** absorption (OD) taken in the monomer **M1** with the emission profile of the NIR-LED-array (LED790-66-60 from Roithner).

Scheme 1 describes the necessary pathways to generate initiating radicals in the redox system comprising the NIR-dye (**Sens**) as electron donating moiety and the iodonium salt with the general cation structure $[A-I-B]^+$ as electron acceptor functioning as radical initiator. These salts with alkyl substitution in 4-position possess a reduction potential (E_{red}) of -0.7 V^{2c} while **S1** exhibits an oxidation potential (E_{ox}) of 0.4 V¹¹, which is similar compared to similar dye structures with barbiturate group at the *meso*-position^{2c}. **S1** possesses an excitation energy (E_{00}) of 1.6 eV derived from the absorption spectrum in **M1** according to the procedure described elsewhere¹³. These data (E_{ox} , E_{red} , E_{00}) allow calculating the free reaction enthalpy of electron transfer ΔG_{el} , Eq. 1, resulting in about -0.5 eV. Thus, this reaction is possible from thermodynamic point of view, which should lead to an almost similar reactivity between **Sens*** and $[A-I-B]^+$. However, the results obtained show that data do not fit in this hypothesis.

$$\Delta G_{\text{el}} = F \cdot (E_{\text{ox}} - E_{\text{red}}) - E_{00} \quad (1)$$

(F : Faraday constant, E_{ox} : oxidation potential, E_{red} : reduction potential, E_{00} : excitation energy)

Equation 1 describes the first reaction steps; that is the formation of the oxidized dye species **Sens**⁺. This cleaves fast to lower molecular weight products¹⁴ and acid¹¹ making the system irreversible. Otherwise, electron back transfer between $[A-I-B]$ and **Sens**⁺ would dominate in such a singlet system resulting in a less efficiency of initiator radical formation.



Scheme 1: Reaction scheme for NIR-initiated radical polymerization based on electron transfer. Excitation of **Sens** results in formation of its first excited singlet state **Sens***. Electrochemical data allow a rough estimate of the HOMO and LUMO energies of **Sens** and the iodonium salt **[A-I-B]⁺**, respectively. Electron transfer from **Sens*** to **[A-I-B]⁺** results in reduction of the iodonium salt and yields the iodyl radical **[A-I-B]•**. This short-living intermediate cleaves with a high efficiency and yields initiating aryl radicals **A•**. The fast decomposition of both **[A-I-B]** and **Sens⁺** results in a decrease of the efficiency of electron back transfer.

Several diaryliodonium salts with distinct substitution pattern were investigated to check if there exists a relation between reactivity and structural. Scheme 2 depicts the different structural variations of the iodonium cations investigated. Nevertheless, all cations shown in Scheme 2 differ regarding their size/molar volume. This may affect transport processes (diffusion) in such crosslinking systems.

	R ₁	R ₂	R ₃	R ₁ '	R ₂ '	R ₃ '
1	H	<i>t</i> -C ₄ H ₉	H	H	<i>t</i> -C ₄ H ₉	H
2	H	<i>i</i> -C ₃ H ₇	H	H	<i>i</i> -C ₃ H ₇	H
3	H	CH ₃	H	H	CH ₃	H
4	H	CH ₃	H	H	<i>i</i> -C ₃ H ₇	H
5	CH ₃	CH ₃	CH ₃	CH ₃	CH ₃	CH ₃
6	<i>i</i> -C ₃ H ₇	<i>i</i> -C ₃ H ₇	H	H	<i>i</i> -C ₃ H ₇	<i>i</i> -C ₃ H ₇
7	H	<i>O</i> - <i>i</i> -C ₈ H ₁₁	H	H	H	H
8	H	<i>O</i> - <i>n</i> -C ₈ H ₁₇	H	H	H	H

Scheme 2. Structural changes of the structural pattern of the iodonium cations investigated

Furthermore, different anions (**X⁻**) were combined with iodonium cations to study how anion changes affect reactivity of the NIR photopolymer comprising the sensitizer **S1**, Scheme 3. In this series, only the **[B(Ph)₄]⁻** anion (**a**) possesses redox potentials allowing to interact with the intermediates (**Sens⁺**) formed resulting in an increase of initiation efficiency^{2c}. Thus, borates should exhibit the best performance. However, the results obtained showed that particular some redox inactive anions derived from super acids¹⁵ resulted in the highest reactivity; that is the **[N(SO₂-CF₃)₂]⁻** anion (**n**) and **[B(CN)₄]⁻** anion (**c**).

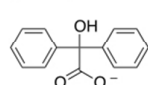
Therefore, the structure of the anions was varied more in detail to obtain a closer pattern between iodonium salt structure and reactivity. Thus borates were first varied regarding their structure (**X⁻**: **a-c**). In contrast to the

tetraphenyl borate **a**, the frontier orbitals of **b** and **c** cannot interact with those of **Sens⁺** according to Scheme 1. Furthermore, hydroxyl substituted carboxylates (**X⁻**: **d-e**), sulfonates (**X⁻**: **i-l**) imides (**X⁻**: **m-n**) or inorganic anions (**X⁻**: **f-h**) were included in the measurements to obtain a deeper insight. The carboxylate anions **d** and **e** were believed to exhibit a sufficient compatibility with the monomers **M1-M4** chosen because they derive from organic materials and should have therefore similar solubility parameters. In addition, the investigation of sulfonates allowed to draw comparisons the anion **i**. Furthermore, some of the ions shown in Scheme 3 were derived from super acids; that is the anion **n** and **c**. Literature reported a huge acidity even on organic solvents¹⁵. Therefore, the use of these anions (**n** and **c**) should improve dissociation of **[A-I-B]⁺X⁻** in the matrix. This should have an impact on matrix compatibility either. Moreover, changes of the cation pattern from a symmetric (**1, 2, 3, 5, 6**) to a asymmetric (**4, 7, 8**) structure should affect the solubility in the monomers.

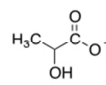
Borates



Hydroxy Substituted Carboxylates



d



e

Inorganic anions

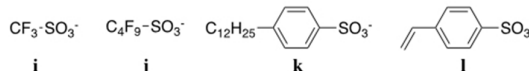


f

g

h

Sulfonates



i

j

k

l

Imids



m

n

Scheme 3. Changes of the structural pattern of the anions introduced in the iodonium salt

Reactivity of the photopolymer

Photo-DSC was applied to investigate the reactivity of the NIR photoinitiator system comprising the sensitizer **S1** and the radical initiator **[A-I-B]⁺X⁻** in the monomers **M1-M4**. This technique was successfully applied in previous investigations^{16a-c} although spectroscopic and shrinkage evaluations are alternatives either^{16d-e}. The maximum of polymerization heat R_p^{\max} roughly describes the reactivity of a photopolymer system^{16a-d} because the system crosslinks during exposure. It is a characteristic point where auto-acceleration and vitrification are equivalent. Thus, diffusion processes control the reactivity and reaction rate constants

change with conversion. Furthermore, termination kinetics often changes from bimolecular termination to termination by initiator radicals at higher conversion degrees^{16a-d}. Nevertheless, choosing of R_p^{\max} forms a reasonable compromise to describe the reactivity because this quantity relates somehow to the initiation efficiency. Though, this is a rough compromise. Figure 2 depicts a characteristic profile obtained during exposure. The larger R_p^{\max} , the higher is the reactivity.

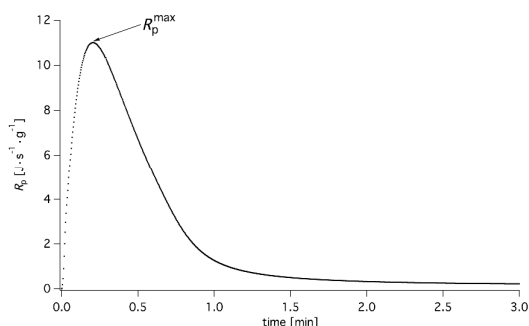


Figure 2. Exothermal heat flow obtained upon exposure of a photopolymer composition with **S1** ($c = 0.83$ mM) and the iodonium salt **1n** ($c = 15$ mM) in the **M1** using a photo-DSC in combination with a NIR-LED array (LED790-66-60 from Roithner).

Figures 3a-c show how change of the anion affects reactivity and while the structure of the cation (**1**) remained unchanged. Both, the bis(trifluoromethylsulfonyl) imide anion (**n**) and tetracyanoborate (**c**) exhibit the highest reactivity and best solubility determined in the hydrophobic monomer **M1**, Figure 3a. There does not exist a clear relation between reactivity and solubility. This follows by comparison of the reactivity of the iodonium salts **1a** and **1h** while these salts exhibit a modest solubility. This unexpected result surprises. It was believed that a high solubility should result in a high reactivity. On the other hand, the solubility of **1j**, **1k**, and **1b** can be considered as high either but these compounds exhibit a lower reactivity in **M1**.

Figure 3b depicts a similar scenario between solubility and reactivity. **1c** possesses the highest reactivity but lower solubility in the higher polar monomer **M2**. On the other hand, the reactivity of **1n** is lower compared to **1c** despite the significant higher solubility of **1n** in **M2**. Similar discrepancies between solubility and reactivity were also obtained in the monomer **M4**.

Furthermore, most of the iodonium salts (**1m**, **1i**, **1h**, **1c**, **1k**, **1a**, and **1g**) exhibit no large differences regarding the reactivity in **M3** (compare SI). The poly(ethylene glycol) chain may cause these changes due to specific solvation effects. Nevertheless, **1n** exhibits also in this monomer a high solubility although the reactivity is slightly smaller compared to the salts mentioned. This shows again that a good solubility is not always mandatory to obtain a high reactivity in the coating.

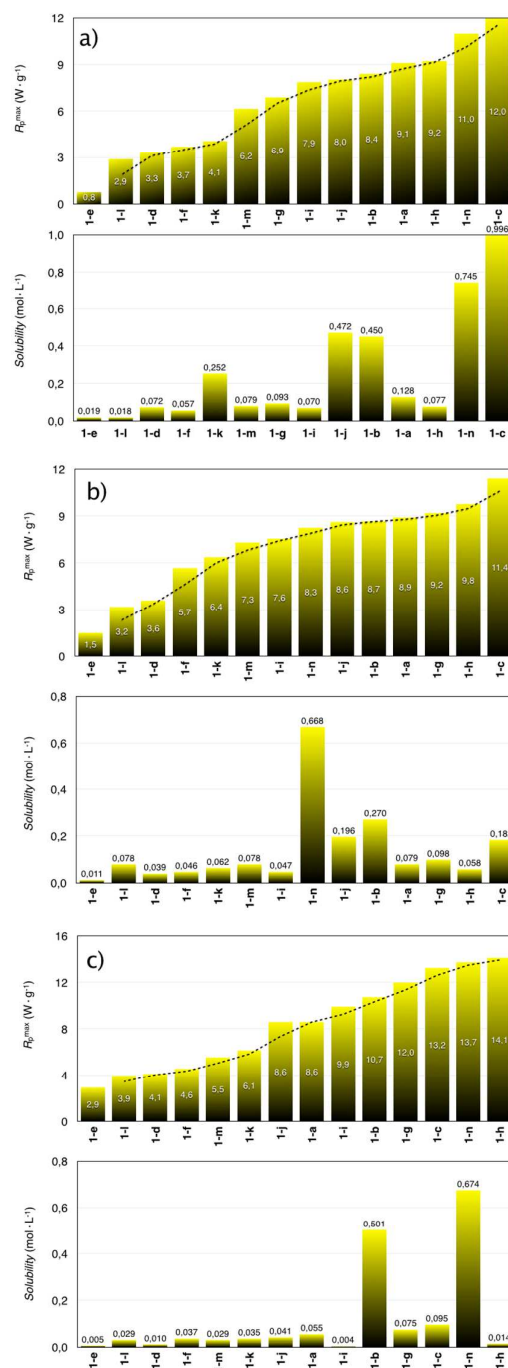
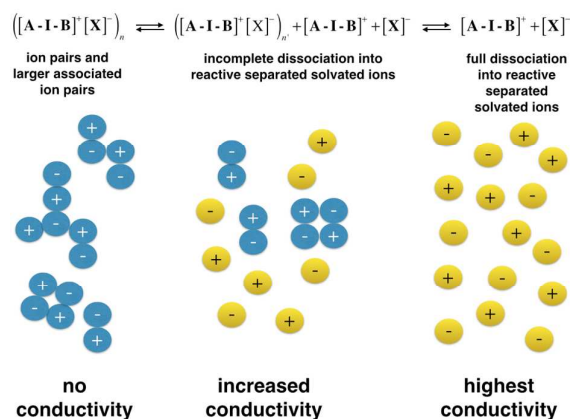


Figure 3. Comparison of reactivity (maximum of polymerization rate R_p determined by photo-DSC with a NIR-LED array) and molar solubility of iodonium salts comprising cation **1** and different anions in the monomers **M1** (a), **M2** (b) and **M4** (c), **S1** concentration: 0.83 mM in **M1**, 0.85 mM in **M2** and 0.9 mM in **M4**; iodonium salt concentration: 15 mM in **M1**, 15.4 mM in **M2** and 16.3 mM in **M4**; exposure was carried out with a NIR-LED array emitting (LED790-66-60 from Roithner) using a photo-DSC for reactivity evaluation.

Influence of conductivity on reactivity

It was believed that dissolution of the iodonium salt results always in the same dissolved species. Therefore, one could expect a correlation between reactivity and solubility. On the

other hand, we found a discrepancy between reactivity and solubility showing that not all dissolved molecules contribute to reactivity. The sketch shown in Scheme 4 depicts formation of different species after dissolution. These are reactive separated solvated ions (\oplus and \ominus), non-dissociated ion pairs ($\ominus\oplus$), dimers ($\ominus\oplus\ominus\oplus$), trimers ($\ominus\oplus\ominus\oplus\ominus\oplus$) or higher molecular aggregates. Only separated solvated ions (\oplus and \ominus) mainly contribute to conductivity according to our results. Thus, conductivity measurements should monitor the availability of separated solvated ions. Higher molecular aggregates do not significantly contribute to the overall conductivity. These assemblies were sometimes called as clusters¹⁷.



Scheme 4: Schematic sketch describing the dissociation of dissolved idonium salts. Left part: no dissociation into solvated ions with no contribution to conductivity (blue), the salts dissolves as dimers, trimers or higher aggregates; Middle part: partial dissociation of dissolved idonium salt into solvated ions (yellow) contributing to conductivity; Right part: complete dissociation of dissolved idonium salt into solvated ions (yellow).

According to Scheme 4, dissolution of the idonium salt results first in formation of associated ion pairs appearing as dimers, trimers or higher aggregates (left part of Scheme 4). These assemblies can further dissociate into reactive separated solvated ions contributing mainly to conductivity. This step presumably occurs incomplete (middle part of Scheme 4) in the monomers chosen while the scenario of complete dissociation (right part of Scheme 4) would probably not be reached in our reactive solvents. There exists still a certain fraction of associated ion pairs, which does not contribute to conductivity. The nature of the surrounding matrix influences this dissociation process and determines the number of available separated solvated ions; that is also the solvated separated cation $[A-I-B]^+$ being available for the reaction with **Sens***. There is still a certain fraction of non-dissociated ion pairs ($m-x$) available that does not contribute to conductivity. An increased conductivity may indicate a higher number of separated solvated idonium ions for electron transfer. Therefore, the reactivity of the NIR-photopolymer system should increase with increasing conductivity.

Equation 2 shows the relation between ion mobility u_i and molar conductivity Λ_m (F = Faraday constant, u_i = ion mobility

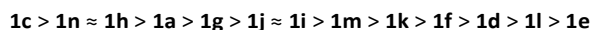
of the i th type of ion, z_i = charge of the i th type of ion, a_i = activity of the i th type of ion, N_a = Avogadro constant). A high ion mobility should result in a high molar conductivity. Nevertheless, this equation was originally derived for diluted aqueous solutions where the concentration was used instead of activity. Description of electrolyte behaviour in organic solvents has not been well understood yet.

$$\Lambda_m = N_a \cdot F (a_+ \cdot z_+ \cdot u_+ + a_- \cdot |z_-| \cdot u_-) \quad (2)$$

Furthermore, the mobility u_i of the i th type of ion is inversely proportional to the friction coefficient f_i of the i th type of ion, Eq. 3. This equation includes Stoke's law in the denominator. Thus, u_i is inversely proportional to the effective radius r_i^{eff} of the ion and the macroscopic viscosity of the matrix. Thus, ions with equal valence magnitudes and equal effective radii should exhibit similar mobility according to Stoke's law. According to this relation, ion mobility and therefore reactivity should increase with decreasing ion size. Uncertain is still the size (r_i^{eff}). Solvated ions also contain a solvation shell and a cloud of ions with opposite charges (electrophoretic effect) whose size determination would require to include microscopic parameters on a molecular scale. Thus, microviscosity effects¹⁸ must be included to understand the transport of ions in a matrix (relaxation effect). Movement of ions repels ions with the same charge but it attracts ions with opposite charge. There exists an ion cloud of unknown size, which must relax to generate new positions for movements of the ions in the matrix. This additionally includes the jump into free volume that was described as microviscosity effect¹⁸.

$$u_i = \frac{|z_i|e}{f_i} = \frac{|z_i|e}{6\pi \cdot \eta \cdot r_i^{\text{eff}}} \quad (3)$$

Figure 4a-c show the dependence between R_p^{max} and Λ_m . First, the nature of the anion was varied while the structure of the cation (**1**) remained constant. As expected, an increase of Λ_m resulted in an increase of R_p^{max} (circles in Figure 4) showing that the model proposed in Scheme 4 might work. The following order was obtained for salts with the cation **1** in **M1**:



This series shows no relation between anion size and conductivity/reactivity (R_p^{max}). The anions **d** and **e** (derived from carboxylates) exhibited together with **l** the lowest reactivity and conductivity although the radius might be comparable with **n** or **b**. A higher conductivity relates to a high ion mobility (Eq. 2), which therefore causes an increase of R_p^{max} , which is proportional to the initiation efficiency.

In the next step, we kept the nature of the anion (**n**) constant and varied the structure of the cation (rectangles in Figure 4). Although there exists no clear relation between cation size, data obtained roughly fit in these plots. Nevertheless, all experiments show that a high conductivity

correlates in most cases with an increased reactivity of the NIR-photopolymer system. Thus, the photoinduced electron transfer requires full dissociation in to well separated ions (Scheme 4) to obtain a high reactivity. Only the anion **b** does not fit in this series. It causes the best conductivity of **1b** in the monomers used (Λ_{\square} in $\mu\text{S}\cdot\text{cm}^2\cdot\text{mol}^{-1}$: 1.21 in **M1**, 0.79 in **M2**, 0.06 in **M4**) while the reactivity (R_p in $\text{W}\cdot\text{g}^{-1}$: 8.4 in **M1**, 8.7 in **M2**, 10.7 in **M4**) is lower compared to **1b**.

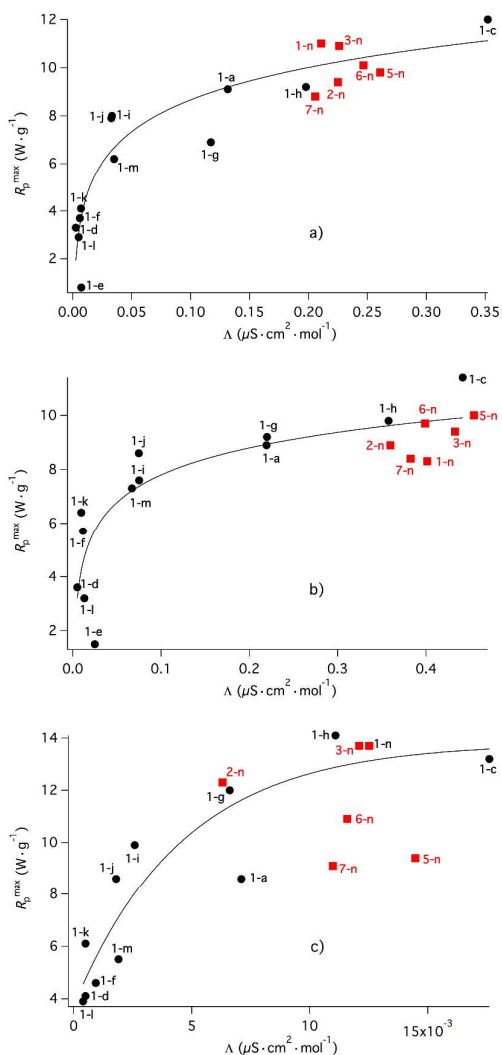


Figure 4: Relation between reactivity (R_p^{\max}) obtained upon exposure of a photopolymer composition with **S1** (concentration: 0.83 mM in **M1**, 0.85 mM in **M2** and 0.9 mM in **M4**) and different iodonium salts (concentration: 15 mM in **M1**, 15.4 mM in **M2** and 16.3 mM in **M4**) in different monomers using a photo-DSC in combination with a NIR-LED array (LED790-66-60 from Roithner) and conductivity of iodonium salts ($c = 10$ mM) in different monomers; a: **M1**, b: **M2**, c: **M4**.

Concentration dependent conductivity measurements were carried out to understand if the iodonium salts could be assigned to either strong (Eq. 4) or weak (Eq. 5) electrolytes in the monomers. The salts **1n-6n** comprise the anion **n** originating from super acids. Thus, one should expect a good dissociation and therefore higher conductivity either.

$$\Lambda_m = \Lambda_m^0 + A \cdot \sqrt{c} \quad (4)$$

(Λ_m = molar conductivity, Λ_m^0 = molar conductivity at infinite concentration, A = constant)

$$\frac{1}{\Lambda_m} = \frac{1}{\Lambda_m^0} + \frac{\Lambda_m \cdot c}{K_a (\Lambda_m^0)^2} \quad (5)$$

(K_a = dissociation constant for the electrolyte $[\text{A-I-B}]^+[\text{X}]^-$)

Concentration dependent studies indicated neither a correlation according to Eq. 4 (Figure 5a) nor to Eq. 5 (Figure 5b). Data treatment of both equations did not result in a linear relationship. Deviations may be caused by a distribution of dissociation steps, which do not occur in one discrete step represented by the dissociation degree x . It follows rather a distribution of many incomplete dissociation steps describing better the scenario.

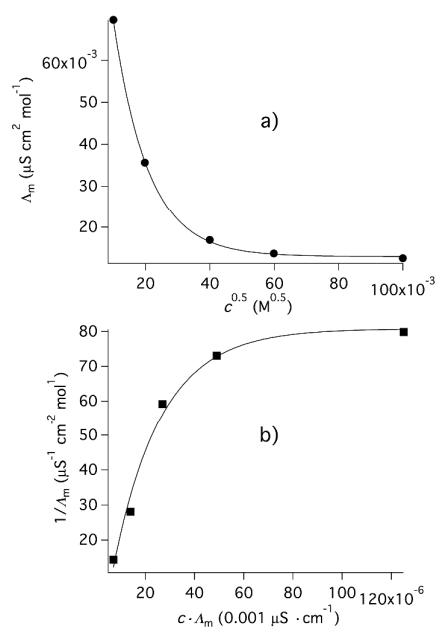


Figure 5: Plot of the conductivity data of **1n** according to (a) Kohlrausch's square law (Eq. 4) and (b) Ostwald's dilution law (Eq. 5).

Influence of the anion on photoinitiator solubility

Iodonium salts comprising the anion **n** exhibit an excellent solubility in **M1-M4**. Change of the cation structure results in some iodonium salts being 1:1 mixable up to a concentration of at least $2000 \text{ g}\cdot\text{L}^{-1}$, Table 1. This is the case for the iodonium salts **2n**, **3n**, and **6n**. Presumably, the cation structure in these compounds reduces the lattice forces in the solid salt resulting in an easier dissolution in the medium. One of the salts (**6n**) appears as viscous oil explaining the well solubility in even extreme non-polar surroundings as well. They belong according to their habitus to the huge class of ionic liquids¹⁸. Furthermore, iodonium salts with the anion **b** exhibit a lower solubility compared to those comprising **n**. Nevertheless, the symmetric salts **1b** and **2b** salts dissolve much better in the

monomers compared to commercially available asymmetric salt **4b**. Nevertheless, these salts (**1b**, **2b**) dissolve even better compared to **1a** bearing $[B(Ph)_4]^-$ as anion. Furthermore, the commercially available iodonium salt **8g** dissolves similar compared to **2b** while **8h** possesses a solubility comparable with **5n**. Moreover, change of the substitution pattern from a *para*-substituted symmetric alkyl compound in **1g** or **1h** to the asymmetric *para*-alkoxy salts **8g** and **8h** does not lead to a significant change of the dissolution behaviour. There has not been known any commercial available iodonium salt that could simply compete regarding the dissolution in the monomers **M1-M4** by comparison with the salts **2n**, **3n** or **6n**. The giant solubility of these salts may be explained by the low coordination capability of the anion **n** and partially by the distorted structure of the cation **6¹⁸**. This may also show why iodonium salts derived from organic acids (**1d**, **1e**) and sulfonic acids (**1l**, **1k**, **1j**, **1i**) possess a significant smaller solubility in the monomers **M1-M4** compared to **1n-7n**.

Table 1: Summary of solubility data of different iodonium salts exhibiting giant solubility (**1n-6n**) and their comparison with other salts (**1b**, **2b**, **4b**, **8g**, **8h**).

[A-I-B] ⁺ [X] ⁻	Solubility (M1) in g·L ⁻¹	Solubility (M2) in g·L ⁻¹	Solubility (M4) in g·L ⁻¹	Solubility (M3) in g·L ⁻¹
1n	501	343	449	576
2n	>2000	>2000	>2000	>2000
3n	>2000	>2000	>2000	>2000
5n	302	174	306	191
6n	>2000	>2000	>2000	>2000
7n	409	325	254	235
1b	482	289	268	209
2b	308	183	146	100
4b	58	58	47	16
8g	39	86	51	51
8h	241	240	144	211

Cytotoxic activity

Some of the iodonium salts shown in Table 1 are new materials. Particular the salts comprising the anion **n** could be of interest for different curing technologies. The use of such chemicals in technologies where the human body could be in contact often requires determination of toxicological data. These data have not been known for the iodonium salts with the anion **n**.

Cytotoxicity represents one important parameter to get a measure of toxicity although this represents only the toxicological behavior of the CHO-9 cells. The MTT-test¹⁰ was chosen to determine cytotoxicity of the iodonium salts **1a** and **1n**, and the infrared dye **S1** in non-irradiated and irradiated samples. Characterization of cytotoxic potential of **1a**, **1n**, and **S1** was grouped in grade scale shown in Table 2. This results in the following cell vitalities; that is grade 0 (non cytotoxic): 100-81%, grade 1 (slightly cytotoxic): 80-71%, grade 2 (cytotoxic): 70-61%, grade 3 (highly cytotoxic): 60-0%. Table 2 summarizes the necessary concentrations to obtain a certain cytotoxicity scale.

Data clearly demonstrate the cytotoxicity of **1a** in the concentration range between 0.026 – 0.26 mg·mL⁻¹. This salt possesses grade 3 at a concentration of 0.026 mg mL⁻¹. On the other hand, **1n** does not cause remarkable cell damages at concentrations up to 0.067 mg·mL⁻¹. Cytotoxicity increases with further concentration increase from 0.134 mg·mL⁻¹ to 0.268 mg·mL⁻¹. Thus, the hydrophobic anion **n** can be considered according to our results as less non-cytotoxic although a higher cytotoxicity exists at higher concentration.

Table 2. Results obtained by MTT assay for the NIR-photoinitiator components **1a**, **1n**, and **S1**.

Grade according to cytotoxic scale	1a (mg·mL ⁻¹)	1n (mg·mL ⁻¹)	S1 (µg·mL ⁻¹)
0	-	≤ 0.067	≤ 0.2
1	-	0.134	0.5
3	≥ 0.026	≥ 0.268	-

The high hydrophobicity and therefore low water solubility of **S1** limits determination of its cytotoxic potential against CHO-9-cells only up to a concentration of 0.5 µg·mL⁻¹. This dye does not exhibit remarkable cytotoxicity in a concentration range between 0.2-0.5 µg·mL⁻¹.

Conclusions

NIR-LEDs with emission at around 780 nm initiate radical photopolymerization of multifunctional acrylic esters comprising a zwitterionic cyanine dye and iodonium salts with distinct substitution pattern. Such photoinitiating systems are interesting because they bleach at the excitation wavelength and open therefore the opportunity to cure coatings with a thickness up to several hundred micrometers. Furthermore, they exhibit an optically open window from the UV into the visible part that allows embedding of functional filter materials covering particular this spectral range.

Moreover, correlation between reactivity and molar conductivity addresses furthermore the question whether there could be more anions available leading to a higher reactivity compared to $[B(CN)_4]^-$. This anion exhibits the best reactivity in most of the monomers investigated. Additional search should go to anions with low coordination capability to obtain a good solubility and reactivity while the salt obtained should not exhibit toxic behaviour. A good solubility is not mandatory to obtain a high reactivity but it is desirable from a practical point of view. These new findings about the behaviour of iodonium salts could be of interest for alternative curing technologies either.

Future research should also focus on the polymethine structure. It has not been clear whether the polymethine dye should bear a barbiturate group in the *meso*-position or not to obtain a reactive composition. Perhaps, the partial negative charges at the oxygen atoms of the barbiturate group may favour interactions with the iodonium cation. This may explain why complete dissociation into separate ions is required to

obtain a high reactivity. Dyes with different substitution in *meso*-position should therefore result in different reactivity.

Previous investigations also assumed that the iodonium salt must contain an oxidable anion, which can be tetraphenyl borate, to make the electron back transfer irreversible from [A-I-B] to the cation radical of Sens⁺. Thus, it was assumed that the tetraphenyl borate fast reacts with Sens⁺ resulting in back formation of Sens with no bleaching. Nevertheless, such a reaction pathway would make the system irreversible because the reaction travels only in one direction. Nevertheless, the system comprising the sensitizer **S1** and radical initiator [A-I-B]⁺X⁻ obviously does not need such an oxidizable anion. Exposure results in fast destruction of **S1** resulting in bleaching at the excitation wavelength and formation of brownish photoproducts. This may explain the capability to cure coatings with larger thickness. Presumably, the very short lifetime of **S1**⁺ results in fast irreversible decomposition of this reactive intermediate.

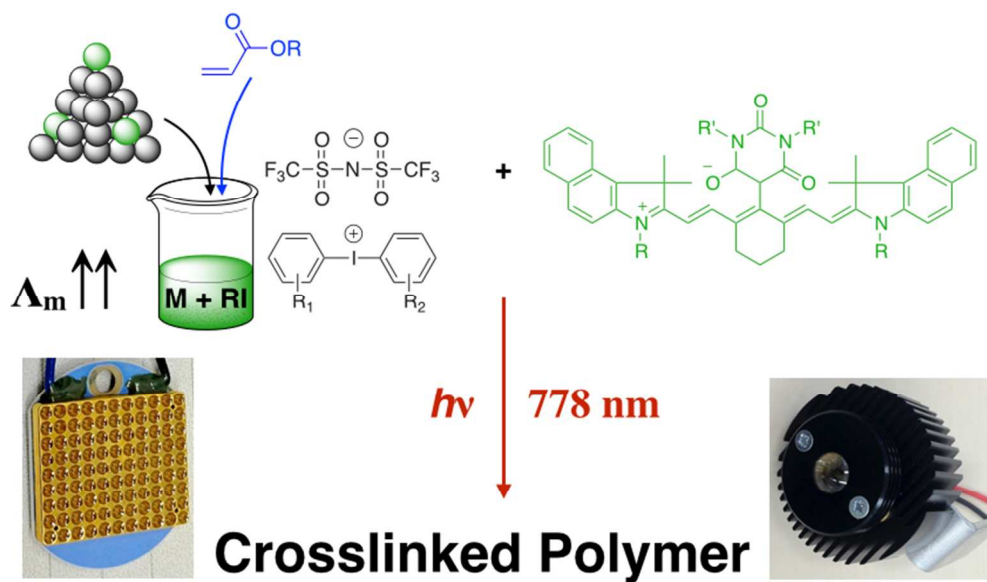
NIR exposure makes this technique interesting for medical and biological applications. This kind of light can deeper penetrate into such materials compared to UV or visible (<650 nm) light. Furthermore, NIR light does not also harm cells while UV light does. Iodonium salts with the anion **n** could be favoured due to their lower cytotoxic response compared to the borate **a**.

Acknowledgements

BS acknowledges the BMWi (ZIM cooperation project KF 2914003BN2). PSP acknowledges the DAAD for a fellowship within the IASTE program. Furthermore, we acknowledge FEW Chemicals GmbH for the **S1** and **8g**, Sartomer for the monomers **M1-M4**, and Hampford Research for the iodonium salts **1g**, **1h**, **8g** and **8h**.

References

- G. Hauck, C. Savariar-Hauck and H.-J. Timpe, *Kodak Polychrome Graphics*, 2000, DE 19906823 A1.
- a) H. Baumann, *Chemie in unserer Zeit* 2014, 48, 14-29. b) H. Baumann, U. Ernst, M. Goetz, A. Griesbeck, M. Oelgemöller, T. Oppenländer, M. Schlörholz and B. Strehmel, *Nachrichten aus der Chemie* 2014, 62, 507-512. c) B. Strehmel, S. Ernst, K. Reiner, D. Keil, H. Lindauer and H. Baumann, *Zeitschrift für Physikalische Chemie* 2014, 228, 129-153. d) B. Strehmel, T. Brömme, C. Schmitz, K. Reiner, S. Ernst, D. Keil, in „Dyes and Chromophore in Polymer Science“, Eds.: J. Lalevée, J.-P. Fouassier, Wiley-ISTE, 2015, pp. 213-249.
- a) J. V. Crivello, *ACS Symp. Ser.* 2003, 847 (Photoinitiated Polymerization), 178-186. b) C. Simpson, H. Baumann and B. Strehmel, *Kodak*, WO2009109579A1, 2009. c) M. Sangermano, N. Razza, J. V. Crivello, *Macromolecular Materials and Engineering* (2014), 299(7), 775-793. d) J. V. Crivello, J. Ma, F. Jiang, H. Hua, J. Ahn, R. Acosta Ortiz, *Macromolecular Symposia* (2004), 215, 165-177. e) W. D. Cook, S. Chen, F. Chen, M. U. Kahveci, Y. Yagci, *Journal of Polymer Science, Part A: Polymer Chemistry* (2009), 47(20), 5474-5487. f) P. Xiao, F. Dumur, J. Zhang, M. Bouzrati-Zerelli, B. Graff, D. Gigmes, J.-P. Fouassier, J. Lalevée, *Journal of Polymer Science, Part A: Polymer Chemistry* (2015), 53(15), 1806-1815. g) J. Zhang, X. Sallenave, T.-T. Bui, F. Dumur, P. Xiao, B. Graff, D. Gigmes, J.-P. Fouassier, J. Lalevée, Jacques, *Macromolecular Chemistry and Physics* (2015), 216(2), 218-227.
- a) C. Grotzinger, D. Burget, P. Jacques and J. P. Fouassier, *Macromol. Chem. Phys.* 2001, 202, 3513-3522. J. Kabatc, M. Zasada and J. Paczkowski, *J. Polym. Sci., Part A: Polym. Chem.* 2007, 45, 3626-3636.
- J.-P. Fouassier, J. Lalevée, *Photoinitiators in Polymer Synthesis*, 2012, Wiley-VCH.
- R. Schwalm, *UV Coatings. Basics, Recent Developments and New Applications*, 2007, Elsevier.
- T. Brömme, J. Moebius, S. Schäfer, C. Schmitz and B. Strehmel, *European Coatings Journal*, 2012, 9, 20-27.
- a) J. G. Huddleston, A. E. Visser, W. M. Reichert, H. D. Willauer, G. A. Broker and R. D., Rogers, *Green Chem.* 2001, 3, 156-164. b) M.-C. Tseng, Y.-M. Liang and Y.-H. Chu, *Tetrahedron Lett.* 2005, 46, 6131-6136.
- a) F. Castellanos, J. Cavezzan, J.-P. Fouassier and C. Priou, *EP562897A1*, 1993. c) C.-W. Cho, T. Phuong Thuy Pham, Y.-C. Jeon, Y.-S. Yun, *Green Chem.* 2008, 10, 67-72.
- T. Mosmann, *Journal of Immunological Methods* 1983, 65, 55-63.
- C. Schmitz, A. Halbhuber and B. Strehmel, poster presentation at the 3rd European Symposium on Photopolymer Science, Vienna, 9-12 September 2014. Solubility of **S1**: 1.9 g·L⁻¹ in **M1**, 1.2 g·L⁻¹ in **M2**, 1.8 g·L⁻¹ in **M3**, and 8.9 g·L⁻¹ in **M4**. These results will be published later in *Progress in Organic Coatings*.
- Additional cationic dye structures were selected from <http://www.few.de/funktionelle-farbstoffe/loesungsmittelloesliche-cyanine/790-819-nm/>.
- H. Mustroph, S. Ernst, B. Senns and A. D. Towns, *Color. Technol.*, 2015, 131, 9-26.
- Exposure of a mixture comprising **S1** and [p-(t-C₄H₉-Ph)₂]⁺[(SO₂-CF₃)₂N]⁻ and their investigation by UPLC-MS-MS-coupling showed bond cleavage along the polymethine chain resulting in formation of lower molecular weight photoproducts. Results will be published in *Photochemical and Photobiological Sciences*.
- A. Kütt, T. Rodima, J. Saame, E. Raamat, V. Mäemets, I. Kaljurand, I. A. Koppel, R.Y. Garlyauskayte, Y. L. Yagupolskii, L. M. Yagupolskii, E. Bernhardt and H. Willner and I. Leito, *J. Org. Chem.* 2011, 76 (2), 391-395.
- a) H.-J. Timpe and B. Strehmel, *Makromol. Chem.* 1991, 192, 779-791. b) H.-J. Timpe and B. Strehmel, *Angew. Makromol. Chem.* 1990, 179, 131-142. c) H.-J. Timpe, B. Strehmel, F. H. Roch and K. Fritzsche, *Acta Polymerica*, 1987, 238-244. d) M. D. Goodner and C. N. Bowman, *Macromolecules*, 1999, 32, 6552-6559. e) J. Liu, G. D. Howard, S. H. Lewis, M. D. Barros and J. W. Stansbury, *European Polymer Journal*, 2012, 48, 1819-1828.
- a) Y. Geng, S. Chen, T. Wang, D. Yu, C. Peng, H. Liu and Y. Hu, *J. Mol. Liq.*, 143, 100 (2008). b) A. Maiti, A. Kumarb and Robin D. Rogers, *Phys. Chem. Chem. Phys.*, 2012, 14, 5139-5146. c) T.-Y. Wu, H.-C. Wang, S.-G. Su, S.-T. Gung, M.-W. Lin and C.-B. Lin, *Journal of the Taiwan Institute of Chemical Engineers*, 2010, 41, 315-325.
- a) B. Strehmel, V. Strehmel and Younes, M., *J. Polym. Sci., Part B: Polym. Phys.* 1999, 37, 1367-1386. b) V. Strehmel, H. Rexhausen, P. Strauch, E. Goernitz and B. Strehmel, *ChemPhysChem* 2008, 9, 1294-1302. c) V. Strehmel, H. Rexhausen, P. Strauch and B. Strehmel, *ChemPhysChem* 2010, 11 (10), 2182-2190.
- P. Wasserscheid and T. Welton, *Ionic Liquids in Synthesis*, Wiley-VCH, 2007.



Efficiency of NIR sensitized radical photopolymerization depends on the dissociation of iodonium salts comprising anions with low coordination capability.
301x176mm (72 x 72 DPI)